Protein kinase C shifts the voltage dependence of KCNQ/M channels expressed in *Xenopus* oocytes

Koichi Nakajo[1,2] and Yoshihiro Kubo[1,2,3]

[1]*Division of Biophysics and Neurobiology, Department of Molecular Physiology, National Institute for Physiological Sciences, Okazaki, Aichi, 444-8585, Japan*
[2]*COE Program for Brain Integration and its Disorders, Tokyo Medical and Dental University, Graduate School and Faculty of Medicine, Bunkyo, Tokyo, 113-8519, Japan*
[3]*Solution Oriented Research for Science and Technology, Japan Science and Technology Corporation, Kawaguchi, Saitama 332-0012, Japan*

It is well established that stimulation of G_q-coupled receptors such as the M1 muscarinic acetylcholine receptor inhibits KCNQ/M currents. While it is generally accepted that this muscarinic inhibition is mainly caused by the breakdown of PIP_2, the role of the subsequent activation of protein kinase C (PKC) is not well understood. By reconstituting M currents in *Xenopus* oocytes, we observed that stimulation of coexpressed M1 receptors with 10 μM oxotremorine M (oxo-M) induces a positive shift (4–30 mV, depending on which KCNQ channels are expressed) in the conductance–voltage relationship (*G–V*) of KCNQ channels. When we applied phorbol 12-myristate 13-acetate (PMA), a potent PKC activator, we observed a large positive shift (17.8 ± 1.6 mV) in the *G–V* curve for KCNQ2, while chelerythrine, a PKC inhibitor, attenuated the shift caused by the stimulation of M1 receptors. By contrast, reducing PIP_2 had little effect on the *G–V* curve for KCNQ2 channels; although pretreating cells with 10 μM wortmannin for 30 min reduced KCNQ2 current amplitude by 80%, the *G–V* curve was shifted only slightly (5 mV). Apparently, the shift induced by muscarinic stimulation in *Xenopus* oocytes was mainly caused by PKC activation. When KCNQ2/3 channels were expressed in HEK 293T cells, the *G–V* curve seemed already to be shifted in a positive direction, even before activation of PKC, and PMA failed to shift the curve any further. That alkaline phosphatase in the patch pipette shifted the *G–V* curve in a negative direction suggests KCNQ2/3 channels are constitutively phosphorylated in HEK 293T cells.

KCNQ channels are low-threshold non-inactivating voltage-gated K^+ channels, most of which have been linked to inherited diseases such as cardiac arrhythmia, benign familial neonatal convulsions and deafness (Jentsch, 2000). Current through KCNQ channels is known as the M-current and is inhibited by the activation of $G_{q/11}$-coupled receptors (Brown & Adams, 1980; Caulfield *et al.* 1994; Marrion, 1997; Haley *et al.* 1998). In sympathetic neurones, for example, M-current amplitude is reduced by stimulating M1 muscarinic acetylcholine receptors (Brown & Adams, 1980).

How the M-current is inhibited has long been an enigma because the complex intracellular signalling pathway via which it is regulated is comprised of numerous components. Recently, however, the M-current was successfully reconstituted by expressing KCNQ channels and M1 receptors in *Xenopus* oocytes and

in mammalian cell lines (Schroeder *et al.* 1998; Wang *et al.* 1998; Selyanko *et al.* 2000; Shapiro *et al.* 2000). Using those expression systems, it was shown that all KCNQ channels can be inhibited by M1 receptor stimulation, and that receptor-induced hydrolysis of phosphatidylinositol-4'5'-bisphosphate (PIP_2) plays a key role in the muscarinic inhibition of KCNQ channels (Suh & Hille, 2002; Loussouarn *et al.* 2003; Zhang *et al.* 2003).

PIP_2 is a negatively charged membrane phospholipid that interacts with positively charged amino acids in the C-terminal cytoplasmic region of the KCNQ channel (Zhang *et al.* 2003; Park *et al.* 2005). A certain amount of PIP_2 is thought to be required to maintain the activity of KCNQ channels, as channels in inside-out patch membranes quickly run-down without application of PIP_2 to the intracellular side (Zhang *et al.* 2003). A similar mechanism has also been observed in other ion channels,

including inward rectifier K^+ channels and voltage-gated Ca^{2+} channels (Huang *et al.* 1998; Wu *et al.* 2002).

Protein kinase C (PKC) has also been thought to play a role in M-current inhibition (Higashida & Brown, 1986). Although its activation by phorbol esters suppresses the M-current, PKC has not been thought to be an essential factor in the channel's inhibition. This is because its effect is only partial in sympathetic neurones and because its activation does not seem to be required for M-current inhibition (Bosma & Hille, 1989; Marrion, 1994). On the other hand, Hoshi *et al.* (2003) recently reported that AKAP150, which is an auxiliary protein that anchors PKC, directly binds to KCNQ2 channels and that interference caused by that binding diminishes M-current inhibition. Although this result suggests that PKC does, indeed, play a role in M-current inhibition, it is still not clear whether it merely facilitates M-current inhibition by PIP_2 or whether it modulates KCNQ channels independently.

The present work shows that M1 receptor stimulation shifts the conductance–voltage (*G–V*) relationship of all KCNQ channels expressed in *Xenopus* oocytes such that the channels opened at more positive voltages; the magnitude of the change varied from channel to channel. The phorbol ester PMA had a similar effect on the KCNQ2 channel, but induced a smaller shift in KCNQ1 channels. Depletion of PIP_2 using wortmannin also induced a shift in voltage dependence, but one that was much smaller than was induced by PMA. We propose that PKC participates in muscarinic receptor-mediated inhibition of the M-current by modulating the voltage dependence of KCNQ channels.

Methods

Molecular biology

The accession numbers for the KCNQ channels used (see Acknowledgements) are AF000571 for human KCNQ1, NM_133322 for rat KCNQ2, NM_031597 for rat KCNQ3 and AF105202 for human KCNQ4. All KCNQ cDNAs were subcloned into the expression vector pGEMHE for *Xenopus* oocytytes or pCXN2 for HEK 293T cells.

Preparation of *Xenopus* oocytes

Xenopus oocytes were collected from frogs anaesthetized in water containing 0.15% tricaine. After the final collection, the frogs were humanly killed. Isolated oocytes were treated with collagenase (2 mg ml^{-1}, type 1, Sigma) for 5 h, after which oocytes of similar size at stage V were injected with approximately 50 nl of cRNA solution and incubated at 17°C in frog Ringer solution. All experiments conformed to the guidelines of the Animal Care Committee of the National Institute for Physiological Sciences.

Two electrode voltage clamp

K^+ currents were recorded with two-electrode voltage clamp using an OC725C amplifier (Warner Instruments, Hamden, CT, USA) and pCLAMP8 software (Axon Instruments, Union City, CA, USA) 2–5 days after cRNA injection. Data from the amplifier were digitized at 2 kHz. The microelectrodes used were drawn from borosilicate glass capillaries (World Precision Instruments, Sarasota, FL, USA) to a resistance of 0.2–1 MΩ when filled with 3 M potassium acetate and 10 mM KCl (pH 7.2). The bath solution (ND96) contained (mM): 96 NaCl, 2 KCl, 1.8 $CaCl_2$, 1 $MgCl_2$ and 5 Hepes (pH 7.4). Oocytes were held at −80 mV and were stepped for 2 s to different test voltages followed by a 250-ms step pulse to −30 mV for recording tail currents. Tail current amplitudes were typically measured as the average value 10–20 ms after the end of the test pulse. All experiments were carried out at room temperature (25 ± 2°C). For the experiments summarized in Figs 1 and 4, we pretreated oocytes with 100 nM thapsigargin (an endo-plasmic reticulum Ca^{2+}-ATPase pump inhibitor) for more than 3 h to deplete the intracellular Ca^{2+} stores and, as a result, inhibit endogenous Ca^{2+}-activated Cl^- channels. That pretreatment with thapsigargin did not affect the muscarinic inhibition of KCNQ channels indicates a rise in intracellular Ca^{2+} is not essential for muscarinic inhibition in *Xenopus* oocytes. If we did not incubate oocytes with thapsigargin, we observed activation of a large Ca^{2+}-activated Cl^- current upon M1 receptor stimulation. However, the current usually disappeared within 1 min and did not affect the inhibition of KCNQ channels.

Patch clamp

cDNAs encoding KCNQ2, KCNQ3 and EGFP (5 : 5 : 1) or KCNQ2 and EGFP (10 : 1) were cotransfected into HEK 293T cells using Lipofectamine 2000 (Invitrogen, Carlsbad, CA, USA). K^+ currents were then recorded using an Axopatch 1D amplifier (Axon Instruments) and pCLAMP8 software (Axon Instruments) 24–36 h after transfection. Data from the amplifier were sampled at 2 kHz. Patch pipettes had resistances of 2–4 MΩ when filled with a solution of the following composition (mM): 140 KCl, 3 $MgCl_2$, 1 $CaCl_2$, 3 EGTA, 10 Hepes, 3 Na_2ATP (pH 7.4). For the experiments summarized in Figs 7*D* and *E* and 8*B* and *C*, 50 U ml^{-1} alkaline phosphatase from calf intestine (Oriental Yeast, Suita, Osaka, Japan) was also included in the pipette solution. The bath solution contained (mM): 150 NaCl, 2 KCl, 2 $CaCl_2$, 2 $MgCl_2$, 10 Hepes, 10 glucose (pH 7.4). Series resistance was compensated by 80%. The voltage-clamp experimental protocols were the same as those used for two-electrode voltage clamp.

Analysis of channel gating

G–V relationships were plotted using tail current amplitudes obtained at −30 mV. Normalized tail currents were fitted using pCLAMP8 software to a two-state Boltzmann equation (Li-Smerin *et al.* 2000; Hille, 2001):

$$G/G_{\mathrm{max}} = \left(1 + e^{-zF(V-V_{1/2})/RT}\right)^{-1},$$

where G/G_{max} is the normalized tail current amplitude, z is the effective charge, $V_{1/2}$ is the half-activation voltage, and T, F and R have their usual meanings.

Mutagenesis

Mutations were introduced into KCNQ2 cDNA using a QuikChange kit (Stratagene, La Jolla, CA, USA) and confirmed by sequencing.

Drugs

Oxotremorine-methiodide (oxo-M), phorbol 12-myristate 13-acetate (PMA), 4α-PMA, chelerythrine chloride and wortmannin were all purchased from Sigma-Aldrich. Stock solutions were made up in DMSO, stored at −20°C, and diluted in the appropriate solution just before use.

Statistical analyses

The data are expressed as means ± s.e.m., with n indicating the number of samples. Differences between means were evaluated using Student's paired or unpaired t tests. Values of $P \leq 0.05$ were considered statistically significant.

Results

Muscarinic activity induces a positive shift in the conductance–voltage relationship of KCNQ channels in *Xenopus* oocytes

In order to reconstitute the M-current in *Xenopus* oocytes, cRNAs encoding KCNQ channels (human KCNQ1, rat KCNQ2, rat KCNQ2 + rat KCNQ3, and human KCNQ4) were injected together with cRNA encoding the porcine M1 muscarinic acetylcholine receptor. Each channel showed a slowly activating, non-inactivating outward current during 2-s depolarization (Fig. 1*A*, left column). When we added 10 μM oxo-M, a muscarinic acetylcholine receptor agonist, to the external bath solution in the absence of thapsigargin, an endoplasmic reticulum Ca^{2+}-ATPase pump inhibitor, large Ca^{2+}-activated Cl^- currents were activated, but they usually disappeared within 1 min (see Methods). Regardless of whether or not cells were pretreated with thapsigargin, KCNQ current amplitudes gradually declined in the presence of oxo-M until reaching a steady level after about 5 min. The effect

of the M1 receptor stimulation seemed relatively mild in *Xenopus* oocytes; even application of the agonist for 10 min failed to fully inhibit KCNQ currents (Fig. 1*A*, right column).

That KCNQ currents retained substantial amplitudes after M1 receptor-mediated inhibition, provided us with the opportunity to analyse the properties of these channels under conditions of muscarinic inhibition. To do so, we recorded tail current amplitudes at −30 mV after 2-s depolarizations and plotted the *G–V* curves obtained before and after M1 receptor stimulation (Fig. 1*B*). The curves were then fitted with a two-state Boltzmann equation (see the equation in Methods). We also compared the maximum tail current amplitude obtained before and after M1 receptor stimulation (Fig. 1*C*). After receptor stimulation, the maximum tail current amplitudes of KCNQ1, KCNQ2 + KCNQ3, and KCNQ4 were, respectively, reduced to 58.5 ± 10.5%, 71.5 ± 8.4% and 39.8 ± 12.8% of the amplitudes seen before M1 stimulation ($n = 5$ for each). By contrast, the maximum tail current amplitude of homomeric KCNQ2 channels was unchanged or even slightly increased after receptor stimulation (108.5 ± 11.6%; $n = 12$).

We also noticed that the *G–V* curves for some KCNQ channels were shifted; that is, they started to activate at a more depolarized potential after M1 stimulation. As shown in Fig. 2*A*, the *G–V* curves for KCNQ2, KCNQ2 + KCNQ3 and KCNQ4 were all substantially shifted to more positive potentials after stimulation. The *G–V* curve for KCNQ1 was also shifted, but only slightly. The corresponding shifts in $V_{1/2}$ (midpoint of the *G–V* curve) were 4.5 ± 1.7 mV (KCNQ1), 10.3 ± 1.5 mV (KCNQ2), 10.4 ± 1.9 mV (KCNQ2 + KCNQ3) and 29.6 ± 5.6 mV (KCNQ4), respectively (Fig. 2*B* and Table 1, $n = 5$ for each). The z-value (effective charge, see the equation in Methods) was slightly decreased for all KCNQ channels (Fig. 2*C* and Table 1).

Although all KCNQ channels were inhibited by M1 receptor stimulation in *Xenopus* oocytes, the characteristics of the inhibition varied from channel to channel. In KCNQ2 channels, for example, maximum current amplitude was unaffected by M1 receptor stimulation, though the *G–V* curve was substantially shifted. Conversely, in KCNQ1 channels the *G–V* curve was shifted only slightly, while the maximum current amplitude was substantially diminished. We therefore decided to focus on KCNQ2 and KCNQ1 channels with the aim of identifying the mechanisms underling the shifts in the *G–V* curve.

PMA induces a positive shift in the conductance-voltage relationship in KCNQ2 channels

PKC is known to be involved in G_q-coupled receptor signalling and may play a role in muscarinic inhibition

(Higashida & Brown, 1986; Hoshi *et al.* 2003). We therefore tested whether PMA, a potent PKC activator, would also induce a positive shift in the *G–V* curves for KCNQ channels. In this experiment, the exogenous M1 receptor was not expressed. After addition of 1 μM PMA to the bath solution, homomeric KCNQ2 current amplitudes at −30 mV gradually declined until reaching a new steady level, usually within 20 min (Fig. 3*A*, inset). After
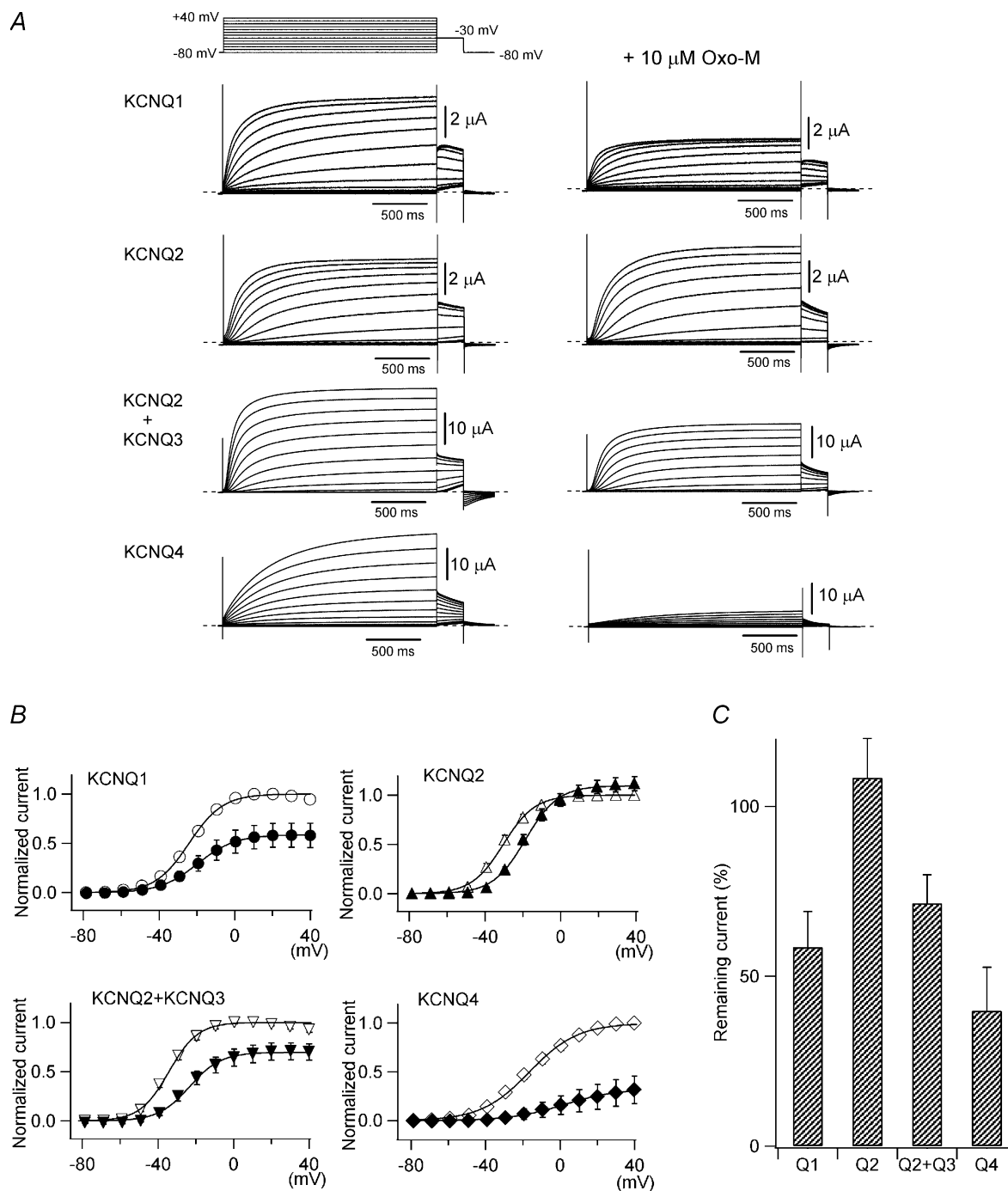
Figure 1. KCNQ/M channels are inhibited by M1 receptor stimulation in *Xenopus* oocytes
KCNQ channels were coexpressed with M1 muscarinic acetylcholine receptors in *Xenopus* oocytes. *A*, representative recordings of currents through KCNQ1 (homotetramer), KCNQ2 (homo), KCNQ2 + KCNQ3 (hetero), and KCNQ4 (homo) channels before and 10 min after the application of 10 μM oxo-M. K$^+$ currents were elicited by voltage steps between −80 and +40 mV followed by a step to −30 mV for tail current analysis. *B*, tail currents at −30 mV before and after muscarinic receptor stimulation are plotted against test potentials. Current amplitudes are normalized to the maximum tail current amplitude before receptor stimulation. Smooth curves were fitted using a two-state Boltzmann function (see Methods). *C*, remaining maximum current amplitudes after muscarinic stimulation are represented as percentages.

Table 1. Changes in $V_{1/2}$ and z for the KCNQ1, KCNQ2, KCNQ2/KCNQ3 and KCNQ4 channel induced by stimulating M1 muscarinic acetylcholine receptors

| | n | $V_{1/2}$ (mV) | | | z | | |
		Before oxo-M	After oxo-M	$\Delta V_{1/2}$ (mV)	Before oxo-M	After oxo-M	Δz
KCNQ1	5	-23.3 ± 1.2	-18.8 ± 1.2	4.5 ± 1.7	2.8 ± 0.1	2.4 ± 0.1	-0.4 ± 0.2
KCNQ2	5	-39.2 ± 1.1	-28.9 ± 1.0	10.3 ± 1.5	4.1 ± 0.1	3.7 ± 0.1	-0.4 ± 0.2
Q2/Q3	5	-34.3 ± 1.1	-23.9 ± 1.6	10.4 ± 1.9	3.2 ± 0.2	2.8 ± 0.1	-0.4 ± 0.2
KCNQ4	5	-15.8 ± 2.3	13.8 ± 5.1	29.6 ± 5.6	1.8 ± 0.2	1.3 ± 0.1	-0.5 ± 0.2

20 min, the current showed slower activation and faster deactivation (Fig. 3*A*). More importantly, the *G–V* curve was positively shifted by 17.8 ± 1.6 mV (Fig. 3*C* and *D*; $n = 5$), an even larger shift than was induced by oxo-M. By comparison, 4α-PMA, an inactive isomer of PMA, induced a *G–V* shift of only 4.4 ± 0.6 mV (Fig. 3*C* and *D*; $n = 6$; $P < 0.001$ *versus* PMA). These results suggest that activation of PKC induces a shift in the *G–V* curve for KCNQ2 in *Xenopus* oocytes. On the other hand, PMA induced a smaller shift in the *G–V* curve for KCNQ1 (5.8 ± 0.6 mV; $n = 6$; Fig. 3*B*, *C* and *D*). As was seen with M1 receptor stimulation (Fig. 2), the *G–V* curve for KCNQ1 channels was little affected by the presence of activated PKC.

To determine whether the *G–V* shift induced by muscarinic stimulation was mediated exclusively via activation of PKC, we applied oxo-M and PMA sequentially to oocytes expressing both M1 receptors and KCNQ channels. In the first experiment, we first applied oxo-M and then PMA. When we applied 10 μM oxo-M to stimulate coexpressed M1 receptors, the *G–V* curve for KCNQ2 shifted 10.3 ± 1.5 mV in 10 min (Fig. 4*A* left, grey triangles; $n = 5$). When we then added 1 μM PMA to the external solution and waited another 20 min, the *G–V* curve was further shifted by another 10.4 ± 1.4 mV (Fig. 4*A* left, filled triangles; $n = 5$). In the second experiment, we first pretreated oocytes with 30 nM PMA for 30 min, after which the averaged $V_{1/2}$ for the *G–V* curves was -18.3 ± 0.7 mV (Fig. 4*A* right, open diamonds; $n = 5$). When we then applied 10 μM oxo-M to the PMA-treated oocytes, we observed no shift (0.0 ± 0.9 mV; Fig. 4*A* right, filled diamonds; $n = 5$). Because PMA had a stronger effect than M1 receptor stimulation on the *G–V* relationship (Figs 2 and 3), PMA might have obscured the effect of oxo-M.
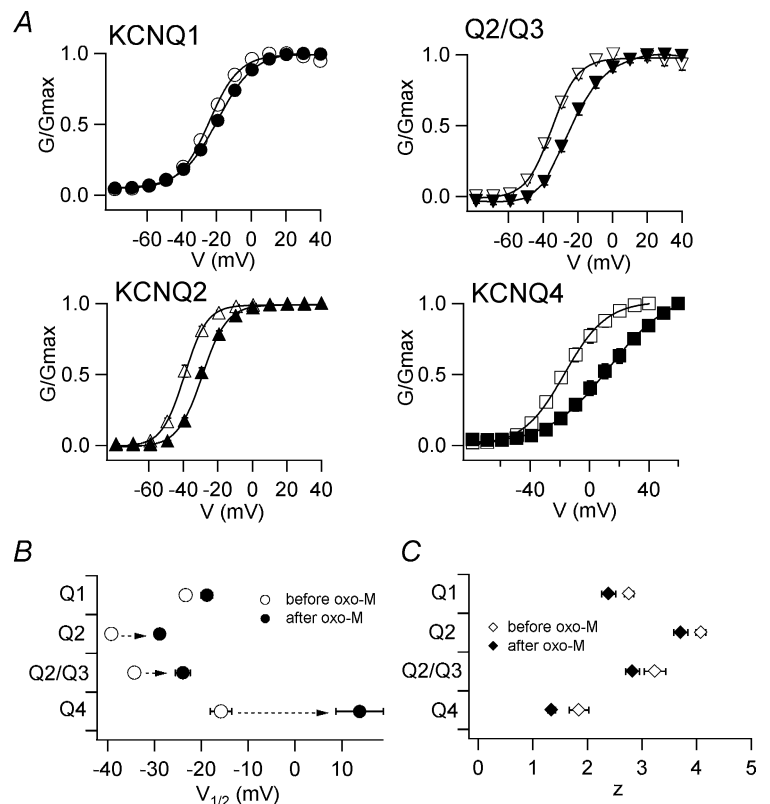
Figure 2. *G–V* curves for KCNQ/M channels are shifted to more depolarized potentials by M1 receptor stimulation
A, *G–V* curves for KCNQ channels before (open symbols) and after (filled symbols) muscarinic stimulation. Smooth curves were fitted using a two-state Boltzmann function. *B* and *C*, $V_{1/2}$ (*B*) and z (*C*) obtained from the two-state Boltzmann function are plotted.

We next tested whether the shift in the *G–V* relationship could be prevented by a PKC inhibitor. After oocytes were pretreated with 20 μM chelerythrine for at least 3 h, the oxo-M-induced shift in the *G–V* curve was significantly

attenuated from 10.3 ± 1.5 mV (control) to 5.4 ± 0.8 mV (Fig. 4*B*; $n = 5$). This suggests that the shift induced by M1 receptor stimulation is due at least in part to activation of a chelerythrine-sensitive PKC subtype.
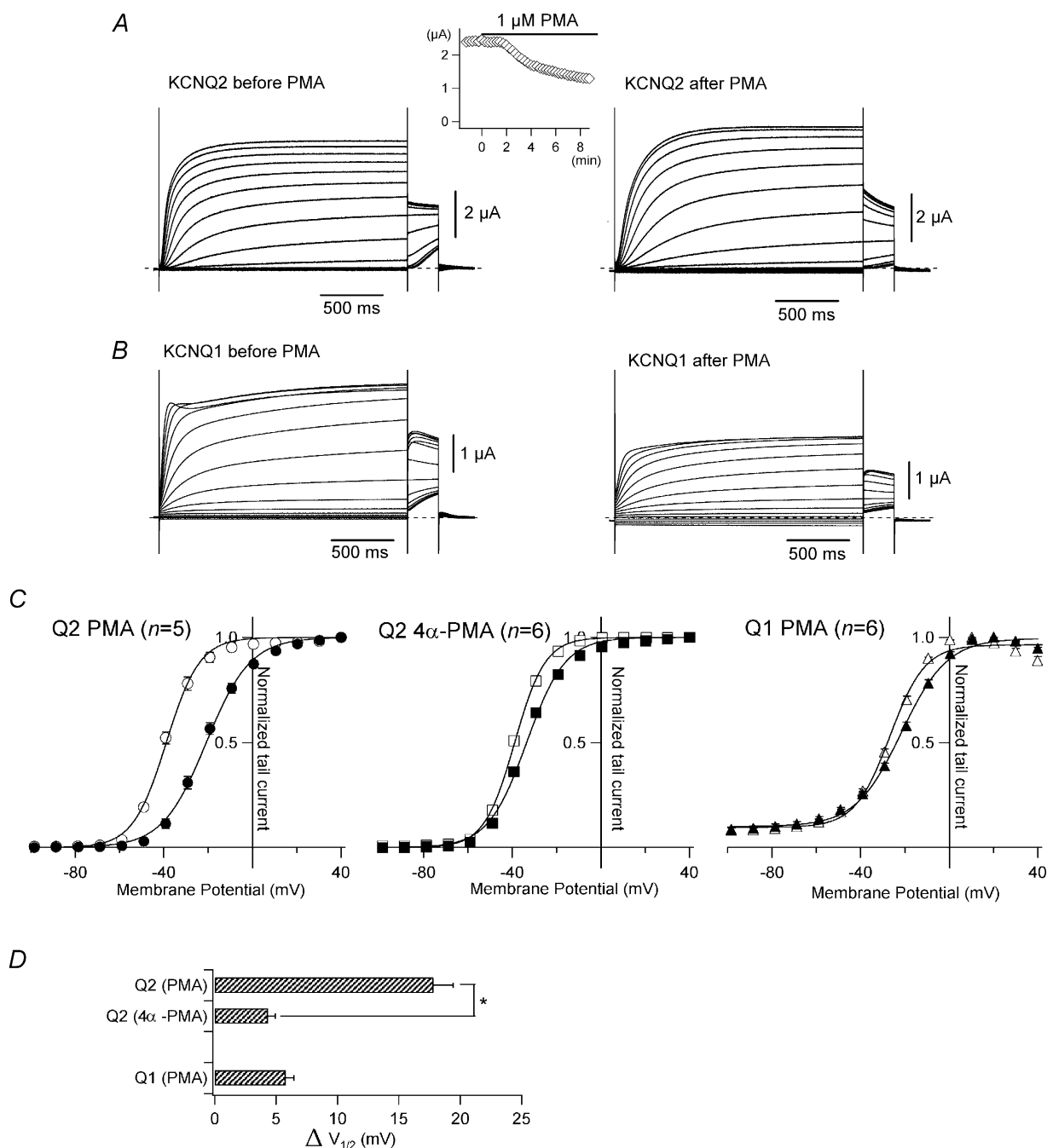
Figure 3. The *G–V* curve for KCNQ2 is shifted by PMA

A, representative current recordings from KCNQ2 channels before and 20 min after application of 1 μM PMA. Currents were elicited by depolarization from -100 to $+40$ mV with a subsequent step to -30 mV for the tail current. The time course of PMA-induced inhibition is shown in the inset. Current amplitudes at -30 mV were plotted against time; 0 min indicates the time at which PMA was applied to the bath solution. *B*, representative current recordings from KCNQ1 channels before and 20 min after application of 1 μM PMA. *C*, *G–V* curves for the KCNQ channels before (open symbols) and 20 min after (filled symbols) application of 1 μM PMA or 1 μM 4α-PMA (inactive isomer of PMA). Smooth curves were drawn by fitting the data with a two-state Boltzmann function. *D*, $\Delta V_{1/2}$ induced by 1 μM PMA or 1 μM 4α-PMA are plotted. The asterisk denotes statistical significance determined using an unpaired Student's *t* test.

Reducing PIP$_2$ reduces KCNQ2 current amplitude and slightly shifts the conductance–voltage relationship of the channel

When G$_q$-coupled receptors are activated, PIP$_2$ is hydrolysed by phospholipase C. Because KCNQ channels are known to require PIP$_2$ to maintain their activity, hydrolysis of PIP$_2$ is thought to be a principle mechanism by which the M-current is inhibited. For instance, with 10 μM wortmannin (known to inhibit both PI4 and PI3 kinases) in the external bath solution, KCNQ channels fail to recover after M1 receptor-mediated inhibition because PIP$_2$ is unable to be re-synthesized (Suh & Hille, 2002; Zhang *et al.* 2003). In addition, incubating oocytes with 30 μM wortmannin reduces KCNQ2/3 current amplitudes by ~95% (Zhang *et al.* 2003). We found that KCNQ2 current amplitudes gradually declined

after addition of 10 μM wortmannin to the external bath solution (Fig. 5*A*), so that they were reduced by approximately 40% after 15 min and by 80% after 30 min (Fig. 5*B*). This is consistent with the idea that KCNQ2 channels in *Xenopus* oocytes require PIP$_2$ for activity, even though the maximum current amplitude was not diminished by M1 receptor stimulation (see Fig. 1). We next pretreated oocytes with 30 nM PMA for 30 min in order to induce a shift in the *G–V* curve before making recordings, after which the cells were placed in external solution containing both 10 μM wortmannin and 30 nM PMA. The PMA-conditioned KCNQ2 currents were also inhibited by wortmannin, declining in amplitude by about 60% within 15 min and 80% within 30 min (Fig. 5*C*). Thus, PMA-treated KCNQ2 channels showing a maximally shifted *G–V* curve still require PIP$_2$ for the activity.
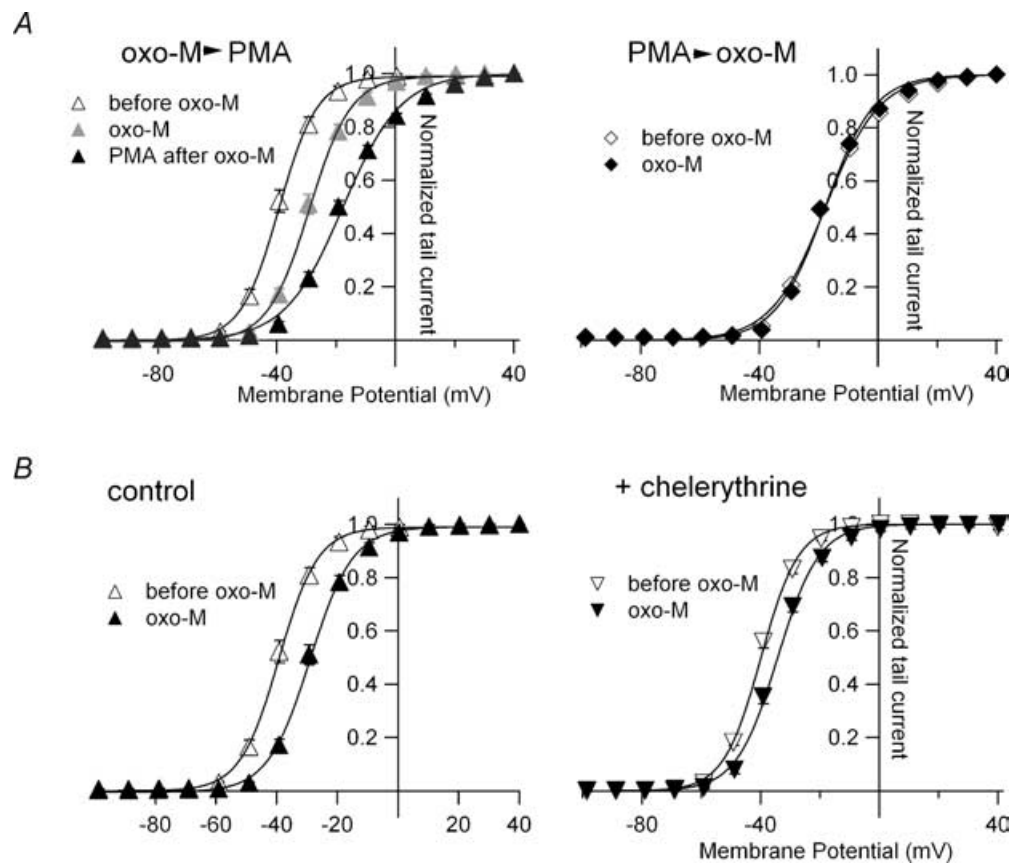
Figure 4. PKC is a main pathway via which receptor stimulation induces *G–V* shifts
A, left, *G–V* curves for KCNQ2 channels obtained before and after sequential application of 10 μM oxo-M and 1 μM PMA. Right, *G–V* curves for KCNQ2 channels before and after application of 10 μM oxo-M to PMA-pretreated cells. Oocytes expressing KCNQ2 channels were incubated with 30 nM PMA for 30 min before the recording. Smooth curves were drawn by fitting the data with a two-state Boltzmann function. *B*, left, *G–V* curves for the KCNQ2 channel before and 10 min after application of 10 μM oxo-M (control). Right, *G–V* curves for the chelerythrine-pretreated KCNQ2 channel before and 10 min after application of 10 μM oxo-M. Oocytes expressing KCNQ2 channels were incubated with 20 μM chelerythrine for 3 h before the recording. Smooth curves were drawn by fitting the data with a two-state Boltzmann function.
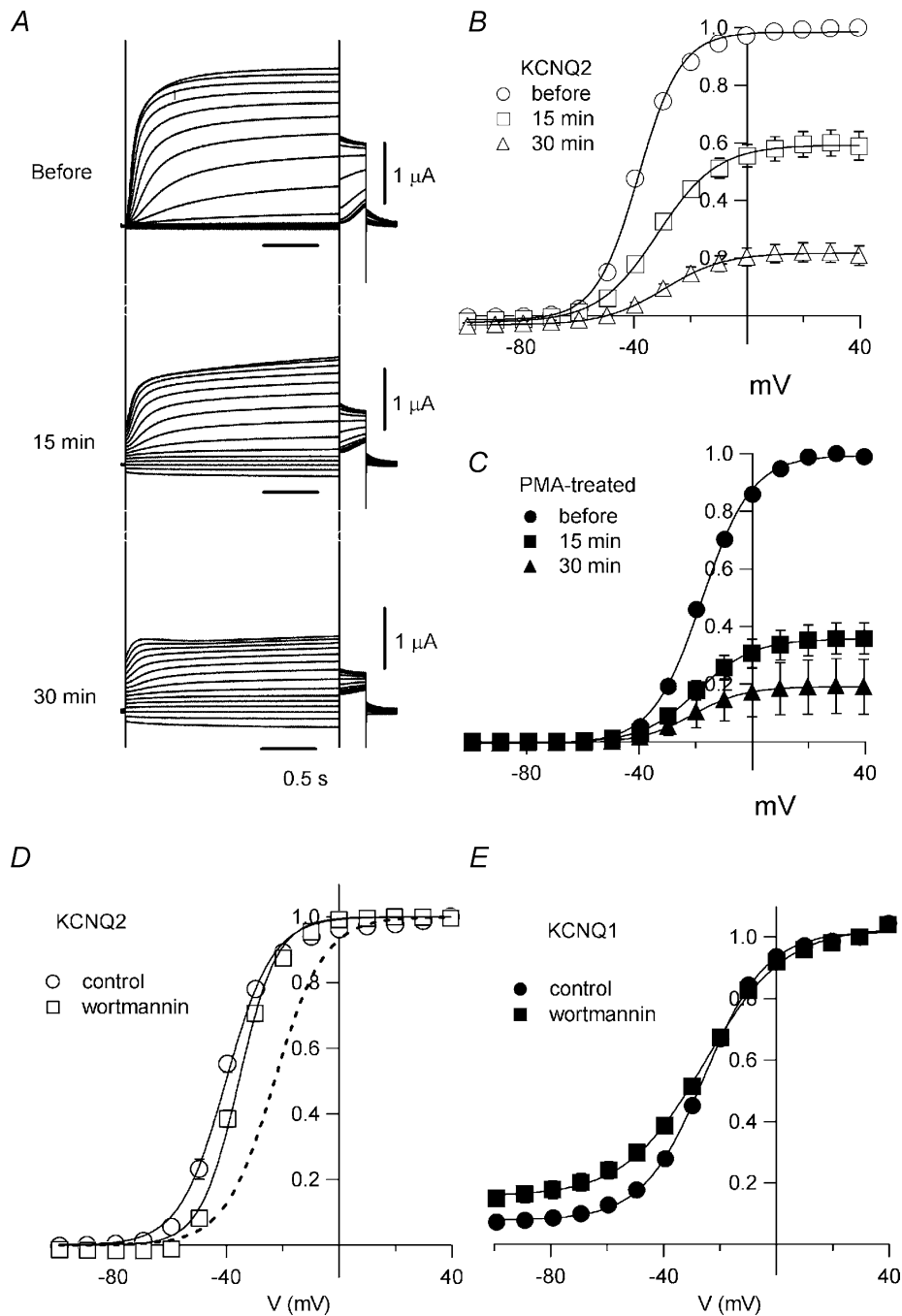
Figure 5. Reduction of PIP$_2$ reduces KCNQ current amplitude and slightly affects *G–V* curves
A, representative current recordings before and 15 min and 30 min after application of wortmannin. *B*, *G–V* curves for KCNQ2 channels before and 15 min and 30 min after application of wortmannin. Forty per cent of the KCNQ2 current was inhibited after 15 min and 80% after 30 min. *C*, *G–V* curves for PMA-treated KCNQ2 channels before and 15 min and 30 min after application of wortmannin. Sixty per cent of the KCNQ2 current was inhibited after 15 min and 80% after 30 min. *D*, *G–V* curves for KCNQ2 channels with (o) or without (□) 30 min pretreatment with 10 μM wortmannin. The dashed curve represents the *G–V* curve for PMA-treated KCNQ2 channels (from Fig. 3*C*). $V_{1/2}$ values were −41.0 ± 1.0 mV (control; $n = 6$), −36.0 ± 0.9 mV (wortmannin; $n = 6$; $P < 0.005$) and −23.1 ± 0.5 mV (PMA; $n = 6$; $P < 0.001$). *E*, *G–V* curve for KCNQ1 channels, which were not affected by PMA (see Fig. 2), were not shifted by wortmannin; $V_{1/2}$ was −25.8 ± 0.7 mV (control; $n = 5$) or −25.3 ± 1.9 mV (wortmannin; $n = 5$; $P > 0.05$), though the KCNQ1 current was inhibited by 78% after incubation for 30 min with 10 μM wortmannin (data not shown).

To determine whether wortmannin would also induce a shift in the $G–V$ relationship, we pretreated oocytes with $10\ \mu\text{M}$ wortmannin for 30 min, which should have caused about 20% of the channels to be inhibited due to a lack of PIP_2 (Fig. 5B). Under those conditions, the $V_{1/2}$ of the $G–V$ curve was -36.0 ± 0.9 mV ($n = 6$), whereas it was -41.0 ± 1.0 mV without wortmannin ($n = 6$; $P < 0.005$) (Fig. 5D). The 5.0-mV shift was significant, but was far smaller than the shift induced by PMA.

KCNQ1 currents also required PIP_2 and were inhibited by 80% after incubating 30 min with $10\ \mu\text{M}$ wortmannin (data not shown). The $G–V$ curve for KCNQ1 was completely unaffected by wortmannin; the $V_{1/2}$ of the $G–V$ curve was -25.8 ± 0.7 mV in the absence of wortmannin ($n = 5$) and -25.3 ± 1.9 mV in its presence ($n = 5$; $P > 0.05$) (Fig. 5E).

Some of KCNQ2 serine-to-aspartate mutants within the A-domain show a positive shift in their conductance–voltage relationship

When M1 receptors are stimulated, some of the serine residues in KCNQ channels are phosphorylated by PKC (Hoshi *et al.* 2003). The KCNQ2 channel protein has a long intracellular C-terminal domain, which contains more than 500 amino acids, including 64 serine and 27 threonine residues. Hoshi *et al.* (2003) identified two serine residues, S534 and S541, that are perhaps responsible for the muscarinic inhibition of KCNQ2 channels. These residues are both located in the middle of the intracellular C-terminal region and are very close to or within the 'A-domain', a region that is highly conserved among KCNQ family proteins and forms the coiled-coil structure needed for tetramerization of KCNQ channels (Fig. 6A) (Jenke *et al.* 2003; Maljevic *et al.* 2003; Schwake *et al.* 2003).

If S534 and/or S541 are the only residues phosphorylated by PKC during muscarinic inhibition, the $G–V$ relationships of single S534A and S541A mutants or a double S534A + S541A mutant should be unaffected by muscarinic inhibition or PKC activation. We found that the $G–V$ curve for the S541A mutant was negatively shifted (~10 mV) under control conditions (Table 2), but that PMA induced a large positive $G–V$ shift in all three S→A mutants tested, as it did with wild-type KCNQ2 (Fig. 6B and Table 2). Apparently, these two serine residues are not the only sites phosphorylated by PKC, which is not surprising given the large number of serine and threonine residues in the intracellular domain of KCNQ2 channels. In addition, these two serine residues are not fully conserved throughout KCNQ family (Fig. 6A). For example in KCNQ4,

A491 corresponds to S534 and phosphorylatable T498 corresponds to S541 while the $G–V$ curve for KCNQ4 was also shifted by muscarinic stimulation (see Figs 1 and 2).

Bearing that in mind, we decided to change our strategy and replaced five serine residues (S534, S541, S563, S567 and S570) in the A-domain with aspartic acid. S563, S567 and S570 are somewhat conserved throughout the KCNQ family except KCNQ1 (Fig. 6A). Because aspartic acid has a negative charge, we expected it to mimic phosphorylated serine and, even before PMA treatment, the $G–V$ curves for the S541D, S563D and S570D mutants were already shifted in a positive direction (Fig. 6C). For example, the $V_{1/2}$ for S541D was -17.7 ± 0.8 mV ($n = 7$), which was close to that for PMA-treated wild-type KCNQ2 channels (the right dotted curve in Fig. 6C; data are the same as in Fig. 3C). S534D and S567D also showed a mild positive shift in their $G–V$ curves (Fig. 6B and C and Table 2), and their averaged current amplitudes were comparable to those seen with the wild-type channel (Table 2).

When PMA was applied, the $G–V$ curve for each mutant showed a further positive shift, although it was not as large as that seen with the wild-type KCNQ2 channel. S541D, S563D and S570D, which all showed a large positive shift before the application of PMA, showed a shift of 9.9 ± 1.0, 6.1 ± 1.4 and 7.6 ± 0.8 mV, respectively, while S534D and S567D, which showed a small shift before treatment, showed a PMA-induced shift of 13.3 ± 1.1 and 17.6 ± 1.4 mV, respectively (Fig. 6B and C and Table 2). It thus appears that phosphorylation of a few residues is sufficient to induce a large positive shift in the $G–V$ curve, even though the protein contains numerous other phosphorylatable sites. S541D and S570D also showed significantly smaller current amplitudes than that of wild-type KCNQ2 after PMA treatment (Table 2). We do not yet have a good explanation for this.

Conductance–voltage relationship of KCNQ2/3 channels is constitutively shifted in HEK 293T cells

Shapiro *et al.* (2000) have already shown that muscarinic stimulation inhibits KCNQ2/3 channels without affecting the voltage dependence in human tsA-201 cells (a derivative of the HEK 293 cell line). In their experiments, however, the PKC inhibitor staurosporine was included in the patch pipette to block the effect of PKC activation. We therefore decided to test whether the $G–V$ curves for KCNQ channels expressed in mammalian cells were also modifiable by PKC activation. In this experiment, both KCNQ2 and KCNQ3 were transfected into HEK 293T cells, after which heteromultimeric KCNQ2/3 channels carried a slowly activating, non-inactivating outward current
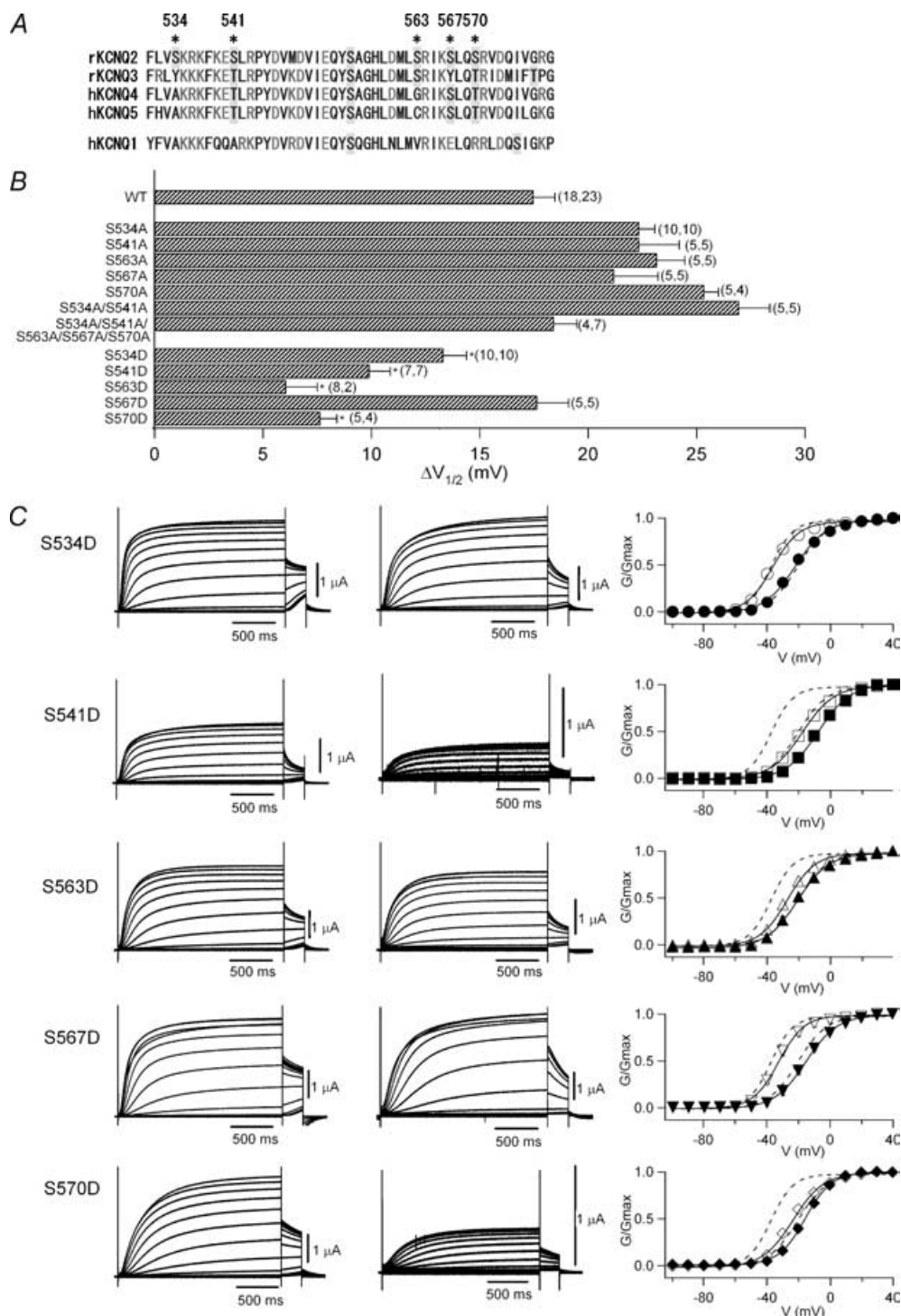
Figure 6. Single S→D mutations within the A-domain of KCNQ2 affects the voltage dependence
A, amino acid sequences of A-domain of rat KCNQ2, rat KCNQ3, human KCNQ4, human KCNQ5 and human KCNQ1. Serine and threonine residues are shaded in grey. Asterisks indicate mutated serine residues in this study. *B*, changes in $V_{1/2}$ ($\Delta V_{1/2}$) after 30-min incubation with 30 nM PMA. Mutants that caused a significant decrease of $\Delta V_{1/2}$ relative to wild-type (WT, top) are indicated with asterisks. The number of measurements (*n*) for each data point is indicated in parentheses; the left number indicating *n* for recordings without PMA incubation and the right number indicating *n* for recordings after 30-min PMA incubation. *C*, representative current traces for S→D KCNQ2 mutants with or without 30-min incubation with 30 nM PMA. Currents were elicited by depolarization from −100 to +40 mV. The *G–V* curve for each mutant with (filled symbols) or without (open symbols) PMA incubation is also shown in the right column. Smooth curves correspond to a two-state Boltzmann function. Dotted curves correspond to fittings obtained with the two-state Boltzmann function for wild-type KCNQ2 channels before and after application of PMA (from Fig. 3*C*).

Table 2. Changes of $V_{1/2}$ induced by PMA for KCNQ2 mutants

	n before PMA	I_{-30mV} (μA) before PMA	$V_{1/2}$ (mV) before PMA	n after PMA	I_{-30mV} (μA) after PMA	$V_{1/2}$ (mV) after PMA	$\Delta V_{1/2}$ (mV)
WT	18	1.66 ± 0.20	-38.2 ± 0.6	23	1.85 ± 0.23	-20.8 ± 0.8	17.5 ± 1.0
S534A	10	2.06 ± 0.20	-39.9 ± 0.5	10	2.15 ± 0.21	-17.6 ± 0.5	22.4 ± 0.7
S541A	5	1.06 ± 0.50	-46.3 ± 0.7	5	3.33 ± 0.59	-23.9 ± 1.7	22.4 ± 1.8
S563A	5	1.65 ± 0.45	-39.7 ± 0.6	5	3.65 ± 0.38	-16.5 ± 1.1	23.2 ± 1.3
S567A	5	0.69 ± 0.18	-39.4 ± 0.2	5	0.84 ± 0.18	-18.2 ± 2.0	21.2 ± 2.0
S570A	5	1.88 ± 0.20	-39.2 ± 0.3	4	2.21 ± 0.53	-13.8 ± 0.6	25.4 ± 0.6
S534A/S541A	5	1.89 ± 0.20	-47.6 ± 0.6	3	1.91 ± 0.36	-20.6 ± 1.3	27.0 ± 1.4
S534A/S541A/S563A/S567A/S570A	5	0.83 ± 0.12	-44.9 ± 0.7	4	1.10 ± 0.42	-26.4 ± 0.8	18.4 ± 1.1
S534D	10	2.13 ± 0.31	-35.5 ± 0.7	10	1.73 ± 0.28	-22.2 ± 0.8	13.3 ± 1.1
S541D	7	0.80 ± 0.17	-17.7 ± 0.8	7	0.17 ± 0.03	-7.7 ± 0.5	9.9 ± 1.0
S563D	8	1.31 ± 0.17	-27.0 ± 0.8	2	0.60 ± 0.33	-21.0 ± 1.2	6.1 ± 1.4
S567D	5	4.04 ± 0.50	-33.2 ± 0.9	5	1.67 ± 0.21	-15.6 ± 1.1	17.6 ± 1.4
S570D	5	1.93 ± 0.35	-23.5 ± 0.5	4	0.19 ± 0.01	-15.9 ± 0.6	7.6 ± 0.8

similar to that seen in *Xenopus* oocytes (Fig. 7*A* left). However, the *G–V* relationship in HEK 293T cells was quite different from that in *Xenopus* oocytes. The $V_{1/2}$ of the *G–V* curve for KCNQ2/3 channels in HEK 293T cells was -23.6 ± 1.4 mV (Fig. 7*B* and *C*; $n = 18$), which is comparable to the $V_{1/2}$ of -21 mV seen previously by Shapiro *et al.* (2000) tsA-201 cells and to the $V_{1/2}$ of -20.8 ± 0.8 mV seen with PMA-treated KCNQ2 channels in *Xenopus* oocytes (right dotted curve in Fig. 7*C*; also see Fig. 3 and Table 2). When we then recorded KCNQ2/3 currents from PMA-treated HEK 293T cells (Fig. 7*A* right), we found that PMA did not elicit a significant reduction in current amplitude or a voltage shift (Fig. 7*B* and *C*); $V_{1/2}$ of the *G–V* relationship in PMA-treated HEK 293T cells was -20.2 ± 1.3 mV (Fig. 7*B* and *C*; $n = 16$; $P = 0.08$).

Because KCNQ2/3 currents in HEK 293T cells were largely insensitive to PMA and the *G–V* curve was similar to that obtained with PMA-treated KCNQ2 channels in oocytes, we hypothesized that KCNQ2/3 channels in HEK 293T cells might already be phosphorylated and therefore the *G–V* curve might already be shifted. If so, dephosphorylation of KCNQ2/3 channels could bring the *G–V* curve back to a more hyperpolarized potential. To test that idea, we added alkaline phosphatase (50 U ml^{-1}) to the patch pipette in order to dephosphorylate KCNQ2/3 channels. After rupture of the cell membrane, the $V_{1/2}$ of the *G–V* relationship gradually shifted in a positive direction (Fig. 7*D* and *E*): $V_{1/2}$ was -23.8 ± 2.1 mV at 0 min (just after the rupture) and -28.0 ± 2.5 mV at 10 min ($n = 9$ for each; $P = 0.01$ by paired *t* test). This implies that KCNQ2/3 channels (or their auxiliary proteins) are constitutively phosphorylated in HEK 293T cells, which could account for the insensitivity of the channels to PMA.

Finally, we examined the behaviour of the S→D mutants in HEK 293T cells. If KCNQ2 channels are constitutively

phosphorylated in HEK 293T cells, and that is the reason why the *G–V* curve for KCNQ2/3 channels was shifted in Fig. 7, the *G–V* curves for the S→D mutants should be similar to that of wild-type KCNQ2 channels. To test that idea, we separately transfected the S541D, S563D or S570D mutant or wild-type KCNQ2 channels into HEK 293T cells. KCNQ3 channels were not cotransfected in this experiment. The S563D mutant was not expressed well in HEK 293T cells and so was not analysed further. The other homomultimeric channels were successfully expressed, and their averaged current amplitudes at -30 mV were 889 ± 188, 147 ± 22 and 502 ± 148 pA for the wild-type ($n = 7$), S541D ($n = 6$) and S570D ($n = 6$) channels, respectively, while the averaged $V_{1/2}$-values were -10.7 ± 1.9, -4.0 ± 1.7 and -5.7 ± 2.7 mV (Fig. 8*A*). The differences in $V_{1/2}$ between the S→D mutants and wild-type KCNQ2 in HEK 293T cells were 6.7 and 5.0 mV for S541D and S570D, respectively, values much smaller than those in *Xenopus* oocytes (20.7 and 14.7 mV for S541D and S570D, respectively; see Fig. 6 and Table 2). This suggests that because of the possible phosphorylation of KCNQ2 channels, the effect of S→D mutation on the *G–V* curve might be obscured in HEK 293T cells.

We also tested whether alkaline phosphatase in the patch pipette would elicit negative shifts in the *G–V* curve for KCNQ2 channels in HEK 293T cells. Along with run-down of the current, the $V_{1/2}$ for wild-type KCNQ2 was shifted toward more negative potentials, from -11.3 ± 2.2 to -17.5 ± 3.0 mV ($n = 4$; Fig. 8*B* and *C*). On the other hand, the current amplitude and $V_{1/2}$ for the S541D mutant were relatively stable with alkaline phosphatase in the patch pipette (from -9.0 ± 0.4 to -6.8 ± 4.5 mV; $n = 3$; Fig. 8*B* and *C*), which supports our hypothesis that S541D mutants mimic phosphorylated KCNQ2 channels.

Discussion

KCNQ channels are inhibited by the activation of G_q-coupled receptors such as the M1 muscarinic acetylcholine receptor, and depletion of PIP_2 and/or the activation of PKC may play a significant role during that process. In the present study, we showed that activation of PKC modulates the gating properties of all KCNQ channels except KCNQ1 in *Xenopus* oocytes. Moreover, whereas the depletion of PIP_2 reduces maximum current amplitude, activation of PKC shifts the *G–V* relationship of the channel. Although KCNQ channels expressed in

HEK 293T cells are insensitive to PMA, our experiment using alkaline phosphatase suggests KCNQ channels are constitutively modulated by phosphorylation in those cells.

Voltage dependence of KCNQ channels

In our present work, we primarily used *Xenopus* oocytes as an expression system. Using this preparation, we found that muscarinic stimulation or PKC activation induced substantial *G–V* shifts for all KCNQ channels except KCNQ1. For example, PMA caused the $V_{1/2}$ of the *G–V*
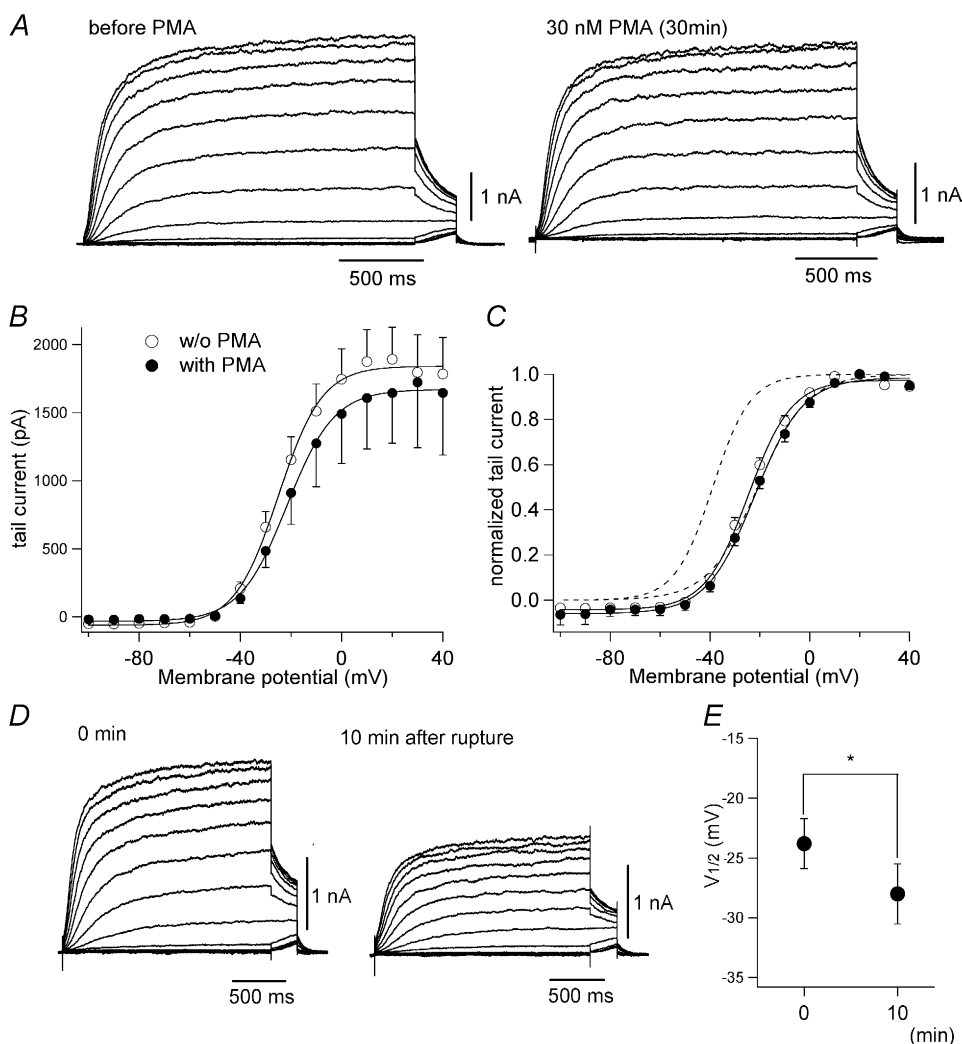
Figure 7. Voltage dependence of KCNQ2/3 channels in HEK 293T cells is insensitive to PMA but sensitive to alkaline phosphatase
A, representative KCNQ2/3 current traces recorded from HEK 293T cells before (left) and after 30-min incubation with 30 nM PMA (right). *B*, mean tail current amplitudes at −30 mV plotted against prepulse voltages. *C*, *G–V* curve for KCNQ2/3 channels with or without PMA treatment. PMA did not shift *G–V* curves in HEK 293T cells. For comparison, dotted curves represent the *G–V* curves for KCNQ2 channels in *Xenopus* oocytes with and without PMA treatment (from Fig. 3*C*). *D*, representative KCNQ2/3 current traces recorded from HEK 293T cells 0 min (left) and 10 min (right) after membrane rupture. The patch pipette contained 50 U ml^{-1} alkaline phosphatase. *E*, change in $V_{1/2}$ induced by alkaline phosphatase is plotted ($n = 9$; $P = 0.01$).

curve for KCNQ2 channels to go from -38.2 ± 0.6 mV to -20.8 ± 0.8 mV (Fig. 3). Muscarinic inhibition also induced a positive shift in the *G–V* curves for KCNQ channels (Figs 1 and 2). By contrast, Shapiro *et al.* (2000) reported that muscarinic inhibition of KCNQ2/3 channels is voltage independent; that is, oxo-M elicited no apparent *G–V* shift in tsA-201 cells. This looks to be a major discrepancy between the two expression systems, but we noticed a few things which may explain this discrepancy. First, with staurosporine in their patch pipette to exclude the effects of PKC activation, those investigators found

that PIP$_2$ does not modulate *G–V* curves. This result is consistent with our finding that depletion of PIP$_2$ does not substantially modulate the voltage dependence of KCNQ2 channels (Fig. 5). Second, *G–V* curves for KCNQ2/3 in tsA-201 and HEK 293T cells look positively shifted even before muscarinic modulation; the $V_{1/2}$ was -21 mV in tsA-201 cells (Shapiro *et al.* 2000) and -23.6 ± 1.4 mV in HEK 293T (Fig. 7). As these values are very close to the $V_{1/2}$ for KCNQ2 channels in PMA-treated *Xenopus* oocytes (Fig. 7*C*), we hypothesize that KCNQ2/3 channels are constitutively phosphorylated in both tsA-201 and
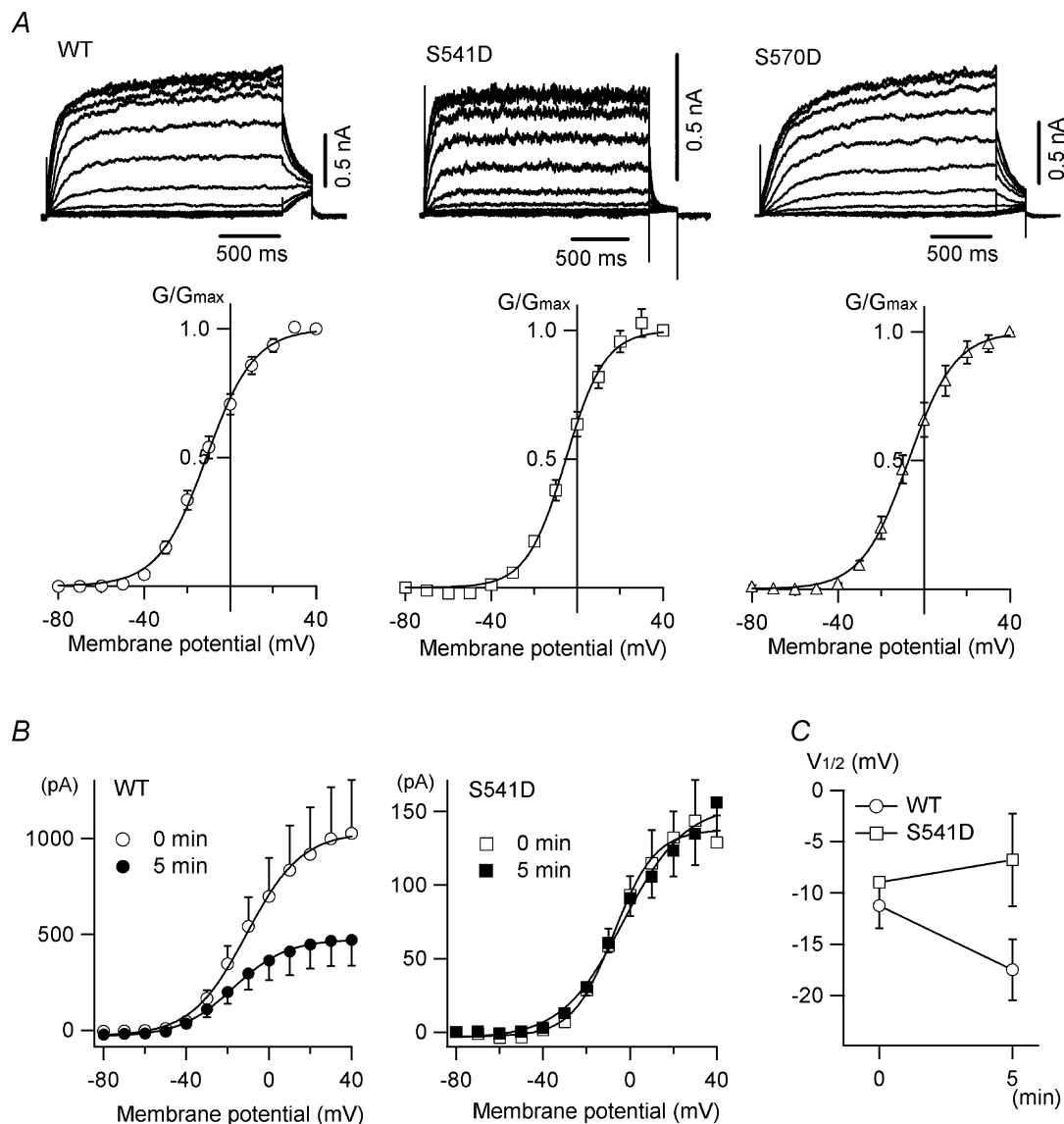
Figure 8. Voltage dependence of wild-type KCNQ2 channels and S→D mutants in HEK 293T cells
A, homomeric wild-type KCNQ2 channels and S541D and S570D mutants were expressed in HEK 293T cells. Shown are representative traces and *G–V* curves acquired from tail currents at -30 mV; $V_{1/2}$ is -10.7 ± 1.9, -4.0 ± 1.7 and -5.7 ± 2.7 mV for wild-type, S541D and S570D, respectively. *B*, tail current amplitudes at -30 mV from KCNQ2 current traces recorded at 0 min (open symbols) and 5 min (filled symbols) after membrane rupture. The patch pipette contained 50 U ml^{-1} alkaline phosphatase. *C*, changes in $V_{1/2}$ induced by alkaline phosphatase are plotted ($n = 4$ for wild-type and $n = 3$ for S541D).

HEK 293T cells. We have no direct evidence showing KCNQ2/3 channels to be constitutively phosphorylated in HEK 293T cells. But consistent with that idea is our finding that addition of alkaline phosphatase to the patch pipette elicited a gradual shift in the $G–V$ curve back to more negative potentials (Fig. 7D and E), presumably due to dephosphorylation of the channels.

Our data, as well as those of Shapiro *et al.* (2000), indicate that the PIP_2 concentration does not have a large effect on the $G–V$ curve. Still, our data show that a reduction in PIP_2 can shift the $G–V$ curve up to 5 mV (Fig. 5), which may explain why inhibition of the shift by chelerythrine is only partial (Fig. 4).

Mechanisms underlying the shift in the *G–V* curves for KCNQ channels

Hoshi *et al.* (2003) showed that serine residues in KCNQ2 channels are phosphorylated when the M1 receptor is stimulated and that muscarinic inhibition of KCNQ2 channels is attenuated in S534A, S541A and R543A mutants. We failed to reproduce a PKC-insensitive mutant even with multiple S→A substitutions (Table 2), which suggests that other phosphorylatable serine residues are responsible for the shift in the $G–V$ curve. It would be difficult to identify all putative phosphorylatable sites in KCNQ2 given that the cytoplasmic C-terminal region of the protein in rat, for example, contains 64 serine and 27 threonine residues. On the other hand, some S→D substitution mutants (e.g. S541D) showed a positively shifted $G–V$ curve in the absence of PMA (Fig. 6), which implies that phosphorylation of a few sites is sufficient to induce a positive shift in the $G–V$ curve.

Other binding proteins could also be targets of phosphorylation by PKC. For instance, in addition to the PKC-anchoring protein AKAP150, a ubiquitous calmodulin is known to bind to KCNQ2 (Wen & Levitan, 2002; Yus-Najera *et al.* 2002), where it senses intra-cellular Ca^{2+} and regulates channel activity (Gamper & Shapiro, 2003). Calmodulin and other auxiliary proteins might be phosphorylated by PKC and in turn modulate the voltage dependence of KCNQ channels.

How might phosphorylation by PKC induce the shift in the $G–V$ curves for KCNQ channels? S534, S541, S563, S567 and S570 all reside in the A-domain, which probably mediates tetramerization of the channel (Jenke *et al.* 2003; Maljevic *et al.* 2003; Schwake *et al.* 2003). In *Shaker* (Kv1) K^+ channels, the N-terminal T1 domain responsible for tetramerization is also involved in channel gating, and a mutation that stabilizes the T1 tetramer also stabilizes the closed state (Cushman *et al.* 2000; Minor *et al.* 2000). If the aforementioned serine residues within the A-domain

of KCNQ channels are truly phosphorylated, a resultant increase in the stability of the domain might affect channel gating as it does in *Shaker* K^+ channels.

Physiological function of PKC during muscarinic inhibition of KCNQ channels

The function of PKC in muscarinic inhibition has long been controversial. In frog sympathetic neurones, smooth muscle cells and NG108-15 neuroblastoma–glioma cells, phorbol esters or diacylglycerols suppress the M-current (Higashida & Brown, 1986; Brown & Higashida, 1988; Pfaffinger *et al.* 1988). In NG108-15 cells, moreover, PKC 19–31 peptide, an effective inhibitor of PKC, elicits a shift in the voltage dependence of the M-current such that the $V_{1/2}$ goes from -34 mV to -44 mV (Schmitt & Meves, 1993). However, because the inhibition induced by phorbol esters or diacylglycerols is partial at most, and because PKC inhibitors fail to prevent receptor-mediated M-current inhibition, PKC has not been considered necessary for muscarinic inhibition (Bosma & Hille, 1989; Chen *et al.* 1994). In the present study, we found that PKC positively shifts the $G–V$ relationship of KCNQ channels; in other words, PKC made KCNQ channels reluctant to open. If the main role of PKC is changing the gating properties of KCNQ channels but not the number of available channels, it is reasonable that PKC only partially suppresses the M-current. By contrast, PIP_2 dramatically affected current amplitude with little change in the gating properties (see Fig. 5). Because PIP_2 is required for the activity of KCNQ channels, there would be no channel activity if PIP_2 were completely depleted. This can be seen in Fig. 5C, where even though PKC was fully activated, some KCNQ current remained and was abolished by wortmannin.

The availability of PKC may differ depending on the cellular or molecular environment, which includes not only PKC itself, but also adaptor and/or auxiliary proteins. Recently, AKAP150 was shown to bind to KCNQ2 channels (Hoshi *et al.* 2003), where it can recruit cytoplasmic PKC to the cytoplasmic domain of KCNQ channels, which should facilitate PKC signalling. It is thus obvious that AKAP150 changes the molecular environment of KCNQ2 channels. On the other hand, the density or concentration of PIP_2 is controlled by the activities of numerous kinases and phosphatases (Andersen, 2005). In the presence of excess PIP_2, activation of the M1 receptor may not be sufficient to suppress KCNQ channel activity. Even in this case, however, PKC could induce a positive shift of the $G–V$ curve. In addition, in frog sympathetic ganglion cells, the response to PMA obscured that to substance P but not that to luteinizing hormone releasing hormone (Bosma & Hille, 1989). This may be indicative of how the cellular environment

around each kind of receptor differs, probably because of its subcellular localization and associated binding proteins.

References

Andersen OS (2005). The 58th annual meeting and symposium of the Society of General Physiologists: lipid signaling in physiology. *J General Physiol* **125**, 103–110.

Bosma MM & Hille B (1989). Protein kinase C is not necessary for peptide-induced suppression of M current or for desensitization of the peptide receptors. *Proc Natl Acad Sci U S A* **86**, 2943–2947.

Brown DA & Adams PR (1980). Muscarinic suppression of a novel voltage-sensitive K$^+$ current in a vertebrate neurone. *Nature* **283**, 673–676.

Brown DA & Higashida H (1988). Inositol 1,4,5-trisphosphate and diacylglycerol mimic bradykinin effects on mouse neuroblastoma x rat glioma hybrid cells. *J Physiol* **397**, 185–207.

Caulfield MP, Jones S, Vallis Y, Buckley NJ, Kim GD, Milligan G & Brown DA (1994). Muscarinic M-current inhibition via $G_{\alpha q/11}$ and α-adrenoceptor inhibition of Ca^{2+} current via $G_{\alpha o}$ in rat sympathetic neurones. *J Physiol* **477**, 415–422.

Chen H, Jassar BS, Kurenny DE & Smith PA (1994). Phorbol ester-induced M-current suppression in bull-frog sympathetic ganglion cells: insensitivity to kinase inhibitors. *Br J Pharmacol* **113**, 55–62.

Cushman SJ, Nanao MH, Jahng AW, DeRubeis D, Choe S & Pfaffinger PJ (2000). Voltage dependent activation of potassium channels is coupled to T1 domain structure. *Nat Struct Biol* **7**, 403–407.

Gamper N & Shapiro MS (2003). Calmodulin mediates Ca^{2+}-dependent modulation of M-type K$^+$ channels. *J General Physiol* **122**, 17–31.

Haley JE, Abogadie FC, Delmas P, Dayrell M, Vallis Y, Milligan G, Caulfield MP, Brown DA & Buckley NJ (1998). The alpha subunit of G$_q$ contributes to muscarinic inhibition of the M-type potassium current in sympathetic neurons. *J Neurosci* **18**, 4521–4531.

Higashida H & Brown DA (1986). Two polyphosphatidylinositide metabolites control two K$^+$ currents in a neuronal cell. *Nature* **323**, 333–335.

Hille B (2001). *Ion Channels of Excitable Membranes*. Sinauer Associates, Inc., Sunderland, MA.

Hoshi N, Zhang JS, Omaki M, Takeuchi T, Yokoyama S, Wanaverbecq N, Langeberg LK, Yoneda Y, Scott JD, Brown DA & Higashida H (2003). AKAP150 signaling complex promotes suppression of the M-current by muscarinic agonists. *Nat Neurosci* **6**, 564–571.

Huang CL, Feng S & Hilgemann DW (1998). Direct activation of inward rectifier potassium channels by PIP$_2$ and its stabilization by G$\beta\gamma$. *Nature* **391**, 803–806.

Jenke M, Sanchez A, Monje F, Stuhmer W, Weseloh RM & Pardo LA (2003). C-terminal domains implicated in the functional surface expression of potassium channels. *EMBO J* **22**, 395–403.

Jentsch TJ (2000). Neuronal KCNQ potassium channels: physiology and role in disease. *Nat Rev Neurosci* **1**, 21–30.

Li-Smerin Y, Hackos DH & Swartz KJ (2000). alpha-helical structural elements within the voltage-sensing domains of a K$^+$ channel. *J General Physiol* **115**, 33–50.

Loussouarn G, Park KH, Bellocq C, Baro I, Charpentier F & Escande D (2003). Phosphatidylinositol-4,5-bisphosphate, PIP$_2$, controls KCNQ1/KCNE1 voltage-gated potassium channels: a functional homology between voltage-gated and inward rectifier K$^+$ channels. *EMBO J* **22**, 5412–5421.

Maljevic S, Lerche C, Seebohm G, Alekov AK, Busch AE & Lerche H (2003). C-terminal interaction of KCNQ2 and KCNQ3 K$^+$ channels. *J Physiol* **548**, 353–360.

Marrion NV (1994). M-current suppression by agonist and phorbol ester in bullfrog sympathetic neurons. *Pflugers Arch* **426**, 296–303.

Marrion NV (1997). Control of M-current. *Annu Rev Physiol* **59**, 483–504.

Minor DL, Lin YF, Mobley BC, Avelar A, Jan YN, Jan LY & Berger JM (2000). The polar T1 interface is linked to conformational changes that open the voltage-gated potassium channel. *Cell* **102**, 657–670.

Park KH, Piron J, Dahimene S, Merot J, Baro I, Escande D & Loussouarn G (2005). Impaired KCNQ1-KCNE1 and phosphatidylinositol-4,5-bisphosphate interaction underlies the long QT syndrome. *Circ Res* **96**, 730–739.

Pfaffinger PJ, Leibowitz MD, Subers EM, Nathanson NM, Almers W & Hille B (1988). Agonists that suppress M-current elicit phosphoinositide turnover and Ca^{2+} transients, but these events do not explain M-current suppression. *Neuron* **1**, 477–484.

Schmitt H & Meves H (1993). Protein kinase C as mediator of arachidonic acid-induced decrease of neuronal M current. *Pflugers Arch* **425**, 134–139.

Schroeder BC, Kubisch C, Stein V & Jentsch TJ (1998). Moderate loss of function of cyclic-AMP-modulated KCNQ2/KCNQ3 K$^+$ channels causes epilepsy. *Nature* **396**, 687–690.

Schwake M, Jentsch TJ & Friedrich T (2003). A carboxy-terminal domain determines the subunit specificity of KCNQ K$^+$ channel assembly. *EMBO Rep* **4**, 76–81.

Selyanko AA, Hadley JK, Wood IC, Abogadie FC, Jentsch TJ & Brown DA (2000). Inhibition of KCNQ1-4 potassium channels expressed in mammalian cells via M1 muscarinic acetylcholine receptors. *J Physiol* **522**, 349–355.

Shapiro MS, Roche JP, Kaftan EJ, Cruzblanca H, Mackie K & Hille B (2000). Reconstitution of muscarinic modulation of the KCNQ2/KCNQ3 K$^+$ channels that underlie the neuronal M current. *J Neurosci* **20**, 1710–1721.

Suh BC & Hille B (2002). Recovery from muscarinic modulation of M current channels requires phosphatidylinositol 4,5-bisphosphate synthesis. *Neuron* **35**, 507–520.

Wang HS, Pan Z, Shi W, Brown BS, Wymore RS, Cohen IS, Dixon JE & McKinnon D (1998). KCNQ2 and KCNQ3 potassium channel subunits: molecular correlates of the M-channel. *Science* **282**, 1890–1893.

Wen H & Levitan IB (2002). Calmodulin is an auxiliary subunit of KCNQ2/3 potassium channels. *J Neurosci* **22**, 7991–8001.

Wu L, Bauer CS, Zhen XG, Xie C & Yang J (2002). Dual regulation of voltage-gated calcium channels by PtdIns(4,5)P$_2$. *Nature* **419**, 947–952.

Yus-Najera E, Santana-Castro I & Villarroel A (2002). The identification and characterization of a noncontinuous calmodulin-binding site in noninactivating voltage-dependent KCNQ potassium channels. *J Biol Chem* **277**, 28545–28553.

Zhang H, Craciun LC, Mirshahi T, Rohacs T, Lopes CM, Jin T & Logothetis DE (2003). PIP$_2$ activates KCNQ channels, and its hydrolysis underlies receptor-mediated inhibition of M currents. *Neuron* **37**, 963–975.